ELSEVIER

Journal of Hazardous Materials B117 (2005) 149–159

Journal of Hazardous Materials

www.elsevier.com/locate/jhazmat

Decomposition of benzene in the RF plasma environment Part II. Formation of polycyclic aromatic hydrocarbons

Shun-I Shih, Ta-Chang Lin*, Minliang Shih

Department of Environmental Engineering, National Cheng Kung University, Tainan, 70101 Taipei, Taiwan

Received 5 February 2004; received in revised form 8 September 2004; accepted 10 September 2004
Available online 8 December 2004

Abstract

This study investigated the characteristics of polycyclic aromatic hydrocarbons (PAHs) formed during the decomposition of benzene (C_6H_6) in radio-frequency (RF) plasma environments. The identification and quantification were accomplished by using a GC/MS for PAHs and an on-line Fourier transform infrared (FT-IR) spectrometer for the reactants and gaseous products. The analytical results show that PAHs were formed in both C_6H_6/Ar and C_6H_6/H_2/Ar systems. In terms of individual PAHs, naphthalene ($C_{10}H_8$) was the predominant species found among the 21 PAHs under all operational conditions, phenanthrene and chrysene are the next. High-ring PAHs did not form easily in the C_6H_6/Ar and C_6H_6/H_2/Ar system, especially at high input power and high C_6H_6 feed concentration ($C_{C_6H_6}$) for the former system. Yields of PAHs with different ring numbers decreased with increasing ring number. At low input power, increasing $C_{C_6H_6}$ would promote yields of PAHs, while adding hydrogen as the auxiliary gas suppressed PAHs formation. Higher input power or addition of oxygen not only effectively suppresses PAHs formation but also completely destroys C_6H_6. Owing to the absence of the principal intermediate species, phenol (C_6H_5OH), from the gas products of C_6H_6/O_2/Ar system, H-abstraction–C_2H_2-addition (HACA) pathway is proposed as the primary mechanism for PAHs formation in the present study. Gas phase distribution of total-PAHs accounts for 20–95.3% at 2% of $C_{C_6H_6}$ among C_6H_6/Ar, C_6H_6/H_2/Ar and C_6H_6/O_2/Ar systems. This study suggests that gas-phase PAHs should not be ignored, particularly in C_6H_6/Ar systems under high input power and high $C_{C_6H_6}$, or in C_6H_6/O_2/Ar systems.

Keywords: Polycyclic aromatic hydrocarbons (PAHs); Radio-frequency (RF); Plasma; Benzene (C_6H_6); Decomposition

1. Introduction

Benzene (C_6H_6), a popular solvent and additive in gasoline, is frequently found in both evaporative emission and automobile exhaust. Earlier works on C_6H_6 destruction were mainly on pyrolysis, and were conducted over a wide range of temperatures and concentrations [1–3]. Bauer and Aten devised a chain mechanism for C_6H_6 pyrolysis [4], involving initiation, chain propagation, companion and termination. Finally, two-ring PAHs (naphthalene, $C_{10}H_8$) should be created during the termination step.

In 1995, Mimura synthesized PAHs from C_6H_6 using shock waves and found that the main products were naphthalene, biphenyl, phenanthrene and chrysene [5]. Sonication of C_6H_6 at room temperature is accompanied by the formation of dark insoluble matter, which is believed to be associated with PAHs formation [6]. Accordingly, PAHs formation always occurred in pyrolytic conditions.

C_6H_6 can be thoroughly decomposed under oxygen-rich environments, for example oxidation and combustion processes [7–13]. However, numerous studies demonstrated that PAHs were the main byproducts of these processes [7,9–10]. Phenol (C_6H_5OH), a reactive species in the atmospheric environment, has always been found in the premixed C_6H_6 flames and plasma environment [7–8,10]. Naturally, phenol is considered an important intermediate for PAHs formation.

* Corresponding author. Tel.: +886 6 275 7575x65829; fax: +886 6 275 2790.
E-mail address: tachang@mail.ncku.edu.tw (T.-C. Lin).

0304-3894/$ – see front matter © 2004 Elsevier B.V. All rights reserved.
doi:10.1016/j.jhazmat.2004.09.030

However, the formation and growth pathway of PAHs is still poorly understood.

PAHs are classified as semi-volatile organic compounds (SVOCs) which exist in the atmosphere as gas-phase or are associated with suspended particulate matter. A better understanding of the formation of PAHs can provide practical benefits owing to the apparent environmental health effect of numerous PAHs.

PAHs are well known for their carcinogenicity and mutagenicity. PAHs are also considered to be precursors of soot formation. The formation and growth mechanism of PAHs in flames has been discussed in many studies [7,9,14–15]. Two mechanisms have been proposed for the PAHs formation by additional rings: (1) H-abstraction–C_2H_2-addition (HACA) mechanism: including successive loss of ring hydrogen atoms and acetylene additions to the ring and ring closure reactions [16]. (2) Phenoxy mechanism: the phenoxy radical (C_6H_5O) is produced under oxidative conditions, and then undergoes ring contraction to create cyclopentadienyl radical (C_5H_5) and CO. The self-reaction of cyclopentadienyl can produce naphthalene [17]. However, some studies have recognized the problem of overestimating the importance of the phenoxy mechanism in flames [7,15]. The H-abstraction–C_2H_2-addition mechanism has further been supported by the study of Wang and Frenklach [16]. H-abstraction activates the C_6H_6 molecule and acetylene addition to propagate molecular growth, which can accurately describe the mass growth of PAHs from C_6H_6 to pyrene, and which has also been confirmed using the B3LYP/4-31G approach with low barriers [14]. Furthermore, HACA mechanism has been employed by McEnally and Pfefferle to clarify the results of PAHs formation [7]. However, the mechanism of PAH formation in flames can differ significantly from that in plasma environments, particularly for reactions without oxygen participation.

PAHs formation and growth in plasma was first reported by Hsieh et al. [18]. Hsieh et al. found considerable quantities of PAHs in the deposition when methyl *tert*-butyl ether (MTBE) was added to the radio-frequency (RF) plasma. However, only deposition on the internal reactor wall was gathered for PAHs analysis, while the PAHs in the gas-phase were ignored in their study. To comprehensively study total PAHs, PAHs in the deposition and gas-phase were all collected for analysis.

The present study aimed to investigate the contents of 21 PAHs species with various $C_{C_6H_6}$ and input powers among C_6H_6/Ar, C_6H_6/H_2/Ar and C_6H_6/O_2/Ar plasma systems. Phase distribution and PAHs yields in rings 2–7 are also discussed.

2. Experimental section

A PAH sampling apparatus and a plasma system were connected to assess the characteristics of PAHs formed during the decomposition of C_6H_6 in the plasma environment. C_6H_6 with 99.6% purity was obtained from Merk Co.

2.1. Plasma system

Similar experimental apparatus of plasma system have been described in greater detail elsewhere [19]. By applying a vacuum, C_6H_6 can easily be transformed into the vapor phase. Flow rates of C_6H_6, H_2, O_2 and Ar were individually metered using calibrated mass flow controllers (Brooks-type 5850E). A total flow rate of 100 sccm ($cm^3\,min^{-1}$, 1 atm, 273 K) entered the mixing vessel and was then introduced into a glass reactor. The operational pressure was always adjusted near 10 Torr before the application of RF plasma. The RF plasma reactor, as illustrated in Fig. 1, was a two-piece cylindrical glass vessel, with inner diameter 4.5 cm and total height 20 cm. The outer copper electrode was 6 cm high, and was wrapped on the plasma reactor and grounded.

An RF plasma generator (CESAR, Dressler) and a matching network (Dressler, Vario Match) supply 13.56 MHz power to the reactor. Before each run, the system was exposed to a vacuum to reduce it to a pressure below 0.01 Torr. An oil diffusion pump was then used to further lower the pressure to 0.001 Torr. The gaseous product species out of the reactor are introduced online into a Fourier transform infrared (FT-IR) spectrometer (Nicolet, Avatar 360) with a 9.6 m path length gas cell (CIC, Ranger) for species identification and quantification.

From a previous study [20], the most influential parameters in this RF plasma system are input power wattage and

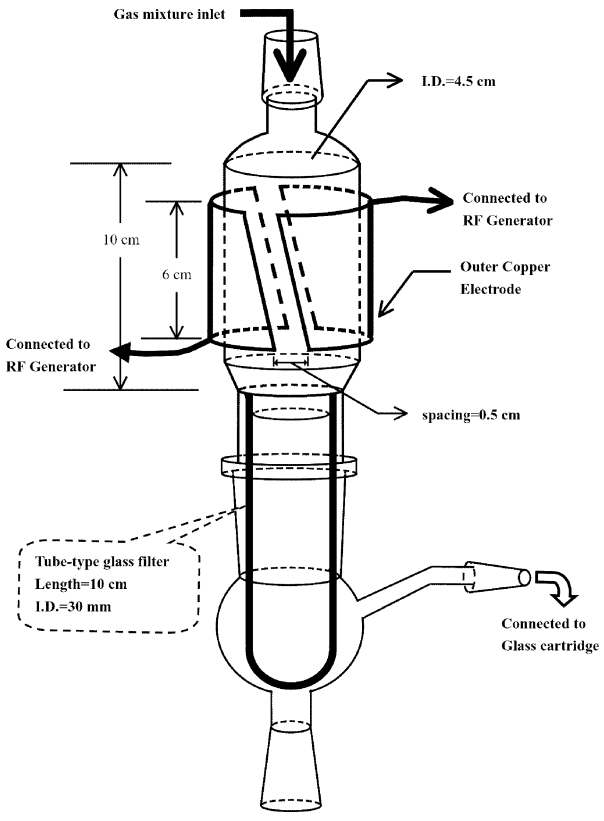

Fig. 1. Plasma reactor.

feed concentration. In this study, the RF plasma system was operated under two specified feed concentrations of C_6H_6, including 1 and 10% for both low input power (40 W) and high input power (90 W). $C_6H_6/H_2/Ar$ and $C_6H_6/O_2/Ar$ at 2% feed concentration of C_6H_6 were also conducted for evaluating the influence of hydrogen and oxygen on PAHs formation. During the experiments involving all operational conditions, a smelly, dark yellow, soot-like materials appeared on the internal wall of the reactor and the filter. This finding resembles the findings of Mimura [5] and of Senken and Castaldi [21].

In this study, the total flow rate was set 100 sccm under all operational conditions. The electron temperature in the plasma zone could exceed 10^3 K, depending on the power input and gas species produced. After the plasma zone, the gas flow temperature was rapidly quenched to below 400 °C. This study calculated the electron temperature in the plasma zone using the computer model; they were 2220, 2280, 2340, 2400, 2450 °C for 5, 10, 20, 40, 60 W, respectively. However, away from the plasma zone, the temperature at the exit of the plasma reactor ranged between 200 and 400 °C, depending on power input. Additionally, the temperatures at the filter for collecting the particle-phase PAHs were 57 and 115 °C with the input power of 40 and 90 W, respectively.

2.2. Sample collection

The glass–fiber thimble (Whatman), with length 10 cm and internal diameter 30 mm, was first connected to the outlet of the plasma zone for collecting particle-phase PAHs, after which the gas-phase PAHs was collected by PUF/XAD-16. The pore size of the glass filter ranged between 0.7 and 1.0 μm, while the glass cartridge packed with 2.5 cm of XAD-16 resin was sandwiched between two 5-cm PUF plugs [22–23]. Silicone glue was used to seal and hold these two pieces of PUF and prevent resin leakage during sampling and extraction [22–23]. Depositions on the reactor wall were extracted with a mixed solvent (*n*-hexane and dichloromethane, v/v = 1:1) and then added to the glass–fiber thimble. Following 8 h of adhesion with the silicone glue, each fresh PUF/resin cartridge was cleaned up by Soxhlet extracted for one day each with distilled water, methanol, dichloromethane, and finally, *n*-hexane for a total of 4 days. Each PUF/resin cartridge was then placed in a vacuum oven at 60 °C for 2 h for drying and evaporating the residual solvent. Before sampling, each PUF/resin cartridge was individually wrapped in hexane-washed aluminum foil and stored in a refrigerator at 4 °C, then transported in a clean screw-capped jar fitted with a Teflon cap liner. Each glass fiber thimble was stored in a prebaked glass box, which was also wrapped with aluminum foil during transportation. Finally, the glass cartridge and the glass–fiber thimble were carefully wrapped with aluminium foil to protect the PAHs from light.

2.3. PAHs analysis

The glass cartridge and glass–fiber thimble were Soxhlet extracted separately using a mixed solvent (*n*-hexane and dichloromethane, v/v = 1:1) for 24 h. The extract was concentrated through purging with ultra-pure nitrogen (flow rate 1.0 L min^{-1}) to 2 mL, followed by a cleanup procedure for removing interferences that would co-elute with PAHs during the gas chromatograph (GC) analyses. The cleanup procedure was performed in a cleanup column (internal diameter 1 cm), which contained roughly 5 g glasswool at the bottom, filled with 17 g 6% deactivated silica gel (mixed with 60 mL *n*-hexane) in the middle section, and topped with 1 cm of anhydrous sodium sulfate. Before cleanup, 60 mL *n*-hexane was added for washing the sodium sulfate and silica gel. Immediately before the sodium sulfate layer was exposed to the air, the elution of *n*-hexane was stopped and the eluant was discarded. During cleanup, the concentrated sample was transferred to the cleanup column, and the column wall was then rinsed twice with 2 mL *n*-hexane, which was also added to the column. The eluant collected from the cleanup procedure was then re-concentrated to 0.50 mL with ultra-pure nitrogen [22–23].

A gas chromatograph (Hewlett-Packard 5890A) with a mass selective detector (MSD) (Hewlett-Packard 5972) was used for the PAH analysis. This GC/MS was equipped with a Hewlett-Packard capillary column (HP Ultra 2–50 m × 0.32 mm × 0.17 μm), and PAHs were qualified using the chosen ion monitoring (SIM) mode [22–23].

Twenty-one PAH compounds were quantified, in the following elution order: naphthalene (NaP), acenaphthylene (AcPy), acenaphthene (AcP), fluorine (Flu), phenanthrene (PA), anthracene (Ant), fluoranthene (FL), pyrene (Pyr), cyclopenta(c,d)pyrene (CYC), benz(a)anthracene (BaA), chrysene (CHR), benzo(b)fluoranthene (BbF), benzo(k)fluoranthene (BkF), benzo(e)pyrene (BeP), benzo(a)pyrene (BaP), perylene (PER), indeno(1,2,3,-cd) pyrene (IND), dibenz(a,h)anthracene (DBA), benzo(b)chrysene (BbC), benzo(ghi) perylene (BghiP), coronene (COR).

3. Results and discussion

3.1. PAHs formation in the C_6H_6/Ar system

3.1.1. Yields and distribution of individual PAH

PAH yield(s) (Y_{PAH}) are defined as the ratio of the collected PAHs mass (μg) to the corresponding C_6H_6 feed mass (g). Table 1 lists the results of Y_{PAH} with various $C_{C_6H_6}$ and input power during the decomposition of C_6H_6 in the C_6H_6/Ar system. Evidently in this table, Nap is the predominant one among the 21 PAHs determined under all operational conditions, accounting for 9.03–12.4% (40 W) and 6.60–32.9% (90 W) of total-PAHs, respectively. The fact that naphthalene is the most abundant species among the 21 PAHs can be attributed to two major factors: (1) it has the simplest chemical structure among all of the PAHs, and (2) it is easily formed by acetylene (C_2H_2) additions with low energy barrier [14]. Also, C_2H_2 itself forms easily in the C_6H_6/Ar system [24].

Table 1
Y_{PAH} with various feed concentration of C_6H_6 and input power during decomposition of C_6H_6 in the C_6H_6/Ar RF plasma environment (μg/g C_6H_6)

PAHs[a]	1% of C_6H_6		10% of C_6H_6	
	40 W	90 W	40 W	90 W
Nap	10.7	3.26	116	6.25
AcPy	1.75	0.50	25.3	0.63
Acp	6.38	4.05	25.6	3.06
Flu	4.90	2.62	135	2.62
PA	4.60	2.97	249	4.09
Ant	0.86	0.51	16.7	0.28
FL	2.50	2.01	103	0.33
Pyr	0.56	7.26	22.8	0.48
CYC	2.85	2.01	2.63	0.12
BaA	6.44	0.90	5.96	0.18
CHR	1.59	7.75	289	0.26
BbF	7.06	1.70	119	0.18
BkF	ND	0.01	ND	ND
BeP	19.7	4.96	50.0	0.30
BaP	2.30	1.69	64.8	0.05
PER	1.53	ND	32.8	0.02
IND	1.51	1.90	18.8	0.05
DBA	9.63	ND	ND	ND
BbC	ND	ND	4.50	ND
BghiP	1.57	2.09	3.31	0.07
COR	0.16	3.52	1.35	0.05
Total	86.6	49.7	1285	19.0

ND: not detected.
[a] Gas- and particle-phase included.

Since Nap formation is the first step in the process through which PAH molecules grow, it is important to examine the relevant mechanism. As previously observed, the chain mechanism proposed by Bauer and Aten can explain Nap formation from C_6H_6 pyrolysis in a shock tube [4]. By calculating the free energy of decomposition of C_6H_6, Cataldo also found that Nap formation could occur in accordance with the following two reactions [6]:

$$2\text{Benzene} \rightarrow \text{naphthalene} + \text{acetylene} + H_2$$

$$2\text{Benzene} \rightarrow \text{naphthalene} + 2\text{C(coke)} + 4H_2$$

In flames, two possible pathways exist via which decomposition of C_6H_6 can produce Nap. Some studies have considered Cyclopentadienyl the dominant pathway for Nap formation [9,25], However, it is not quite certain [13]. Additionally, in C_6H_6-doped methane flames, premixing increased Cyclopentadienyl radical (C_5H_5) because of C_6H_6 doping, implying the importance of Cyclopentadienyl pathway. However, C_6H_6 doping also caused the decline of phenylacetylene (C_8H_6) and Nap. C_8H_6 was the most important intermediary in the HACA mechanism, and McEnally and Pfefferle [7] proposed that HACA was the main mechanism for Nap formation in flames, while the Nap produced through cyclopentadienyl self-reaction could be ignored.

As described in the experimental section, a dark yellow-to-brown deposition (coke), as described by Cataldo [6], was formed during the experiment in the C_6H_6/Ar system examined in this study. This study also found abundant C_2H_2 elsewhere [24]. Thus, Nap formation could occur in accordance with the reaction formulas proposed by Cataldo. Phenol was absent from the spectrum analyses because no oxygen was provided. Thus, Nap formation can be interpreted based on the HACA mechanism, which was well applied in pyrolytic or oxidative conditions. However, energetic electrons generated in the C_6H_6/Ar system could play a similar role to oxygen in inducing self-reaction of cyclopentadienyl for Nap formation [7].

$$2C_5H_5 \rightarrow C_{10}H_8 + H_2$$

Phenanthrene and chrysene are another two dominant species. At 40 W of input power, the Y_{PAH} of these species increased from 4.60, 1.59 μg/g C_6H_6 to 249, 289 μg/g C_6H_6, respectively, as $C_{C_6H_6}$ increased from 1 to 10%. Their percentage of total-PAHs increased from 5, 2% to 19, 22%. At 90 W of input power, Y_{PAH} varied from 2.97, 7.75 μg/g C_6H_6 to 4.09, 0.26 μg/g C_6H_6 as $C_{C_6H_6}$ was raised from 1 to 10%. Their contribution to total-PAHs varied from 6, 16% to 21.5, 1.4%. These analytical results indicate that, high $C_{C_6H_6}$ significantly increased yields of PA and CHR at low input power. Meanwhile, at high input power, sufficient energy resulted in low yields of PA and CHR, and thus $C_{C_6H_6}$ insignificantly affected yields of PA and CHR.

On the other hand, when the input power was raised from 40 to 90 W, the Y_{PAH} of PA and CHR varied from 4.60 and 1.59 μg/g C_6H_6 to 2.97 and 7.75 μg/g C_6H_6 at 1% of $C_{C_6H_6}$, whereas their percentages of total-PAHs increased from 5 and 2% to 6 and 16%. At 10% of $C_{C_6H_6}$, Y_{PAH} decreased from 249 and 289 μg/g C_6H_6 to 4.09 and 0.26 μg/g C_6H_6, their percentage of total-PAHs changed from 19 and 22% to 21.5 and 1.3%, respectively. These results indicate that the input power does not significantly affect yields of PA and CHR at low $C_{C_6H_6}$. Whereas, at high $C_{C_6H_6}$, high input power significantly reduces their yields. Based on the above, this study concluded that PA and CHR form more easily at low input power (as 40 W) and high $C_{C_6H_6}$ (as 10%), this result displays good agreement with the synthesis of PAHs from C_6H_6 using shock wave (room temperature: 290 K, liquid C_6H_6, projectile velocity: 100–1140 m/s) [5], both of which exhibit high yields of PA and CHR. This finding indicates that similarities exist between the reactions of C_6H_6 in environments containing plasma and shock wave.

From the perspective of toxicity, benzo(a)pyrene, dibenz(a,h)anthracene and benzo(b)fluoranthene have the highest toxic equivalency factors (TEFs): 1, 1 and 0.1, respectively [26]. Thus, their yields and distributions deserve further investigation. As displayed in Table 1, at 1% of $C_{C_6H_6}$, when input power was raised from 40 to 90 W, Y_{PAH} of BaP, DBA and BbF decreased from 2.30, 9.63 and 7.06 μg/g C_6H_6 to 1.69, ND and 1.70 μg/g C_6H_6. At 10% of $C_{C_6H_6}$, Y_{PAH} decreased from 64.8, ND and 119 μg/g C_6H_6 to 0.05, ND and 0.18 μg/g C_6H_6, respectively. The above observation results reveal that Y_{PAH} of BaP, DBA and BbF were significantly

less at high input power than at low input power, especially at high $C_{C_6H_6}$ (10%).

On the other hand, when $C_{C_6H_6}$ was increased from 1 to 10%, at 40 W of input power, Y_{PAH} of BaP and BbF increased from 2.30, 7.06 μg/g C_6H_6 to 64.8, 119 μg/g C_6H_6, respectively, and DBA decreased from 9.63 μg/g C_6H_6 to ND; regarding 90 W of input power, Y_{PAH} of BaP, DBA and BbF decreased from 1.69, ND and 1.70 μg/g C_6H_6 to 0.05, ND and 0.18 μg/g C_6H_6, respectively. The above results imply that high input power impedes the formation of BaP, DBA and BbF. This finding is similar to those for PA and CHR, which also formed more easily at low input power and high $C_{C_6H_6}$.

For high-ring PAHs, most 5- to 7-ring PAHs did not form easily at high input power, except for BaP (5-ring), BbF (5-ring) and DBA (6-ring). Additionally, Table 1 shows that the plasma environment did not favor the formation of high-ring PAHs such as BaP, particularly at high input power and high $C_{C_6H_6}$. This study concludes that energetic plasma impedes PAHs formation. On the other hand, at high $C_{C_6H_6}$, PAHs forms only at the low electron density.

3.1.2. Influence of C_6H_6 concentration on PAHs formation

For the reactions in this system, higher feed concentration of reactants generally increases the product concentration. Table 1 shows that at low input power (40 W), as $C_{C_6H_6}$ was raised from 1 to 10%, except for CYC, BaA and DBA, whose Y_{PAH} decreased insignificantly, 18 PAHs species increased, along with total-PAHs, from 86.6 to 1285 μg/g C_6H_6. The increase in total-PAHs was approximately 15 fold, whereas at high input power (90 W), as $C_{C_6H_6}$ was raised from 1 to 10%, only Nap, AcPy, PA and PER increased, while the remaining PAHs species decreased, as did total-PAHs, from 49.7 to 19.0 μg/g C_6H_6.

The above observation results demonstrate that high $C_{C_6H_6}$ does not increase Y_{PAH} at high input power. Table 1 also shows that regardless of whether $C_{C_6H_6}$ was 1 or 10%, the Y_{PAH} of individual or total-PAHs was very low, implying that input power (90 W) is sufficient for decomposing C_6H_6 to carbon deposition or gaseous products, but does not favor PAHs formation. Investigating the trend of Y_{PAH} at such low levels is unimportant.

In this RF plasma environment, suitable mean free path should be allowed to accelerate the energetic electrons to effectively collide with the target molecule, ion, or atom. At high $C_{C_6H_6}$ (10%) and 40 W of input power (corresponding to a power density 0.42 W/cm^3), a lack of adequate mean free path and energy led to ineffective collisions among reactants. Thus, C_6H_6 could not be completely decomposed into a gaseous product, and instead reacted to form PAHs (as Table 1). Meanwhile, at 90 W (corresponding to a power density 0.94 W/cm^3), energetic electrons were produced to enhance C_6H_6 decomposition to massive gaseous products, for example, H_2, CH_4, C_2H_4, and C_2H_2, and PAHs formation and growth was suppressed.

3.1.3. Effects of input power on PAHs formation

Mimura [5] reported that high energy conditions promoted the formation of PAHs from C_6H_6 by impact shock. Hsieh et al. [18] also found that PAHs formation in the deposition was easier under high input power in the MTBE/Ar RF plasma environment. Meanwhile, the influence of high temperature on PAHs has also been found in the diesel engine exhaust, where higher temperature enhances PAH decomposition and reduces PAH concentration [27]. The same trend was found during the decomposition of C_6H_6 in the RF plasma. Based on the same $C_{C_6H_6}$, the Y_{PAH} of individual PAHs were considerably lower at high input power (90 W) than low input power (40 W) (see Table 1).

Generally, the pyrolysis reaction is an endothermic reaction, which requires high temperature levels (800–1200 °C) [28]. Based on the experimental results of Shih et al. [19], higher input power can result in higher temperature, and by extrapolation, the estimated temperature could reach 800–1200 °C at 90 W. Additionally, the temperature of energetic electrons in the RF plasma can even exceed 8200 K [29–30]. Higher temperature favors low-ring PAH formation [31–32]. Furthermore, the low-ring PAHs could decompose to gaseous products. This scenario is clearly verified by the experimental results, as shown in a parallel study [24], in which numerous gaseous products, particularly C_2H_2, were identified. Hydrogen, though not detectable by FT-IR, can also exist in significant amount, as noted below. Such information demonstrates that higher input power was not favorable for ring growth, contradicting the findings of Hsieh et al. First, the different reactants (C_6H_6 versus MTBE, O is contained in MTBE) may be the major cause of the entirely different results. The mechanism through which PAHs was produced from different reactants could be markedly different and complicated, especially in terms of oxygen effects. Second, the input power used in the present study was so much higher (90 W > 70 W) that the C_6H_6 ring ruptured and formed C1–C2 gaseous products, along with small quantities of low-ring PAHs, for example Nap (2-ring) and AcPy (3-ring), which closely resemble the observation results for the impact wave technique [5].

3.1.4. Yields of PAHs with various ring numbers

Fig. 2 shows Y_{PAH} for which various ring numbers were generated during C_6H_6 decomposition in the C_6H_6/Ar RF plasma environment. Clearly, levels of Y_{PAH} are much lower at 90 W (B) than at 40 W (A). This fact reveals that higher input power suppressed PAHs formation, mainly because of energetic electrons. From the above result, higher input power is a good choice for reducing the formation of carcinogenic or mutagenic PAHs when C_6H_6 is to be destroyed in an RF plasma environment.

Additionally, the calculations of Wang and Frenklach [33], which supported the hypothesis that reactions of multi-ring aromatic species are in principle similar to those of benzene and phenyl, PAHs formation is associated with the addition of rings. From the standpoint of probability, it becomes

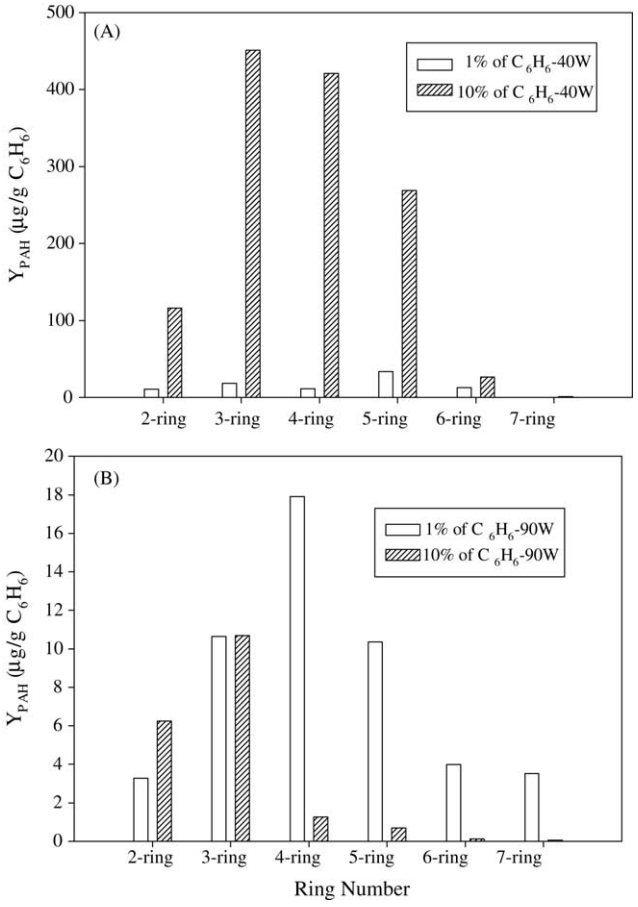

Fig. 2. Y_{PAH} of various ring number during decomposition of different feed concentration of C_6H_6 in the C_6H_6/Ar RF plasma environment.

increasingly difficult to form larger rings. Fig. 2(A) clearly shows that Y_{PAH} decreased with increased ring number at low input power (40 W). Notably, both (A and B), Y_{PAH} of naphthalene was smaller than that of 3-, 4- or 5-ring. As noted by Mimura [5], considering the relatively lower boiling point (218 °C) and tendency to sublime during the analysis, the determined yields for Nap are probably below the actual ones.

3.2. Formation of PAHs in reducing plasma

As previously described, two mechanisms are proposed for elucidating PAHs formation, and the HACA mechanism is considered the most likely pathway for the C_6H_6/Ar system. In this mechanism, the H-atom participates in the HACA mechanism through the H-abstraction reaction, which activates the C_6H_6 molecules. The addition of C_2H_2 then propagates the growth of PAHs molecules. Several studies on C_6H_6 pyrolysis have demonstrated significant hydrogen production at different temperatures [1,3,34–35]. Also, C_2H_2 forms easily in the C_6H_6/Ar system [24]. Thus hydrogen and C_2H_2, which were involved in the PAHs formation, were thought to originate from C_6H_6 decomposition in the C_6H_6/Ar system. Converting C_6H_6 to Nap only requires small energy barriers [14], and so was not the rate-determining step for additional

Table 2
Y_{PAH} of 2% feed concentration of C_6H_6 and 40 W input power during decomposition of C_6H_6 in the C_6H_6/Ar, C_6H_6/H_2/Ar and C_6H_6/O_2/Ar RF plasma environment (μg/g C_6H_6)

PAHs[a]	40 W		
	C_6H_6/Ar	C_6H_6/H_2/Ar (18% H_2)	C_6H_6/O_2/Ar (15% O_2)
Nap	185	156	3.12
AcPy	53.8	8.23	0.51
Acp	57.4	32.3	2.42
Flu	193	205	2.99
PA	319	255	3.03
Ant	25.7	14.8	0.22
FL	141	34.0	0.29
Pyr	49.9	8.76	0.33
CYC	10.5	8.49	0.05
BaA	253	1.76	0.09
CHR	18.2	118	0.03
BbF	155	26.7	0.28
BkF	ND	ND	0.07
BeP	70.0	25.0	0.08
BaP	107	19.8	0.01
PER	65.0	ND	ND
IND	13.0	0.16	ND
DBA	96.9	16.1	ND
BbC	ND	ND	ND
BghiP	9.14	ND	ND
COR	5.34	0.12	1.27
Total	1827	930	14.8

ND: not detected.
[a] Gas-phase and particle-phase included.

ring mechanism. Hydrogen amounts are believed to be the constraining factor for PAHs formation in the C_6H_6/Ar system.

Using 18% of H_2 as the auxiliary gas, this study investigates Y_{PAH} and its distribution at 2% of $C_{C_6H_6}$ and 40 W of input power in the C_6H_6/H_2/Ar and C_6H_6/Ar system (as Table 2). In the C_6H_6/H_2/Ar system, Nap, PA and CHR, which belong to 2- to 4-ring PAHs, were the predominant species, and their Y_{PAH} accounted for 16.7, 27.4 and 12.7 %, respectively, of total-PAHs. Meanwhile, BaP, DBA and BkF, which were more toxic, accounted for 2.13, 1.73 and 0 %, respectively. As for the 19 individual PAHs, they were significantly lower in the C_6H_6/H_2/Ar than in the C_6H_6/Ar system, except for Flu and CHR. Regarding the PAHs ring number, Y_{PAH} decreased with increased ring number in both the C_6H_6/Ar and the C_6H_6/H_2/Ar systems (as shown in Fig. 3). The above result implies that H_2 addition impeded the formation of large PAHs in the RF plasma.

The H/C molar ratio in the feed increased considerably with the addition of 18% H_2. Simultaneously, carbon became deficient, creating a hostile environment for the formation of PAHs which have low H/C ratios ranging from 0.83 (AcP, $C_{12}H_{10}$) to 0.5 (COR, $C_{24}H_{12}$). As a result, small and hydrogen-rich molecules, for example CH_4, C_2H_6, C_2H_4 and C_2H_2, were formed preferentially. The above result was confirmed via a parallel study [24], which showed that addition

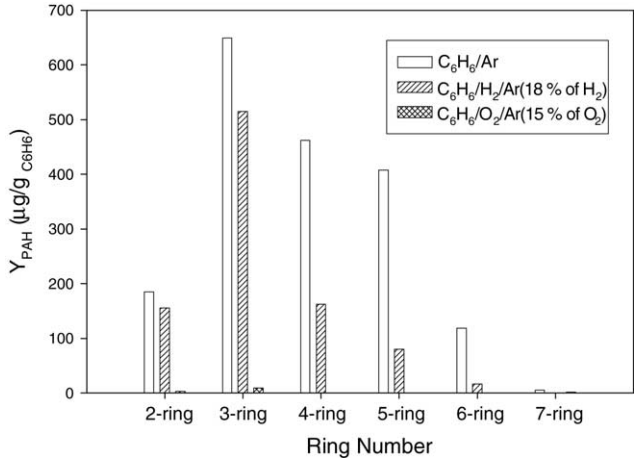

Fig. 3. Y_{PAH} of various ring number during decomposition of 2% of C_6H_6 at 40 W in the C_6H_6/Ar, C_6H_6/H_2/Ar, C_6H_6/O_2/Ar RF plasma environments.

of H_2 can promote the formation of hydrogen-rich species, particularly those of higher H/C species, CH_4 and C_2H_6.

3.3. Effect of O_2 addition

Phenol (C_6H_5OH) can be formed either through attack of hydroxyl radical and oxygen atom on C_6H_6 or by H-atom addition to phenoxy [13,15]. Phenol is a major product formed from combustion or oxidation of C_6H_6 under both atmospheric pressure and low-pressure conditions [7,10,11,36]. Generally, non-thermal plasma (NTP) is a source of gas-phase free radical ($O(^1D)$, $O(^3P)$, $OH^\bullet$) and other active species [37]. Consequently, this study hypothesized that some phenol should be formed in the C_6H_6/O_2/Ar system. The fact that reaction of C_6H_6 with O_2 can produce phenol in the RF plasma has already been confirmed in the study by Tezuka and Yajima [36]. However, no phenol was detected in this C_6H_6/O_2/Ar system.

Fig. 4 illustrates the FT-IR spectra of gaseous products in the C_6H_6/O_2/Ar system. In Fig. 4(A), the operational conditions comprised 2% $C_{C_6H_6}$, 40 W input power and 15% O_2, and the O_2/C_6H_6 ratio was 7.5. Only trace CH_4 (43 ppm) was observed in the gaseous products and 14.8 μg/g-C_6H_6 of PAHs was formed (Table 2) in addition to CO_2, CO and H_2O. In Fig. 4(B), the operational conditions were 1% of $C_{C_6H_6}$, 20 W of input power and 5% of O_2, and the O_2/C_6H_6 ratio was 5. Phenol was not found in this situation either. These observation results show that phenol was not produced under the operational conditions in this study. Accordingly, the mechanism of phenoxy pathway through which PAHs were formed is excluded. The above result implies that the reaction of C_6H_5 (phenyl radical) with O_2 was not the main pathway for PAHs formation in the C_6H_6/O_2/Ar system. Instead, the formation of trace PAHs probably resulted from the HACA pathway.

As observed for the combustion of C_6H_6 by Tregrossi et al., significant amounts of PAHs were formed at the end of the main oxidation ozone; and subsequently their concentration decreased significantly in the burned gas region [10]. Phenol is a highly reactive species. Once phenol is produced in the C_6H_6/O_2/Ar system, it can rapidly react with active radicals to produce stable compounds. Therefore, the pathway of the destruction of C_6H_6 by the gaseous radicals can be represented as: [37]

$$C_6H_6 + O(^3P) \text{ or } OH^\bullet \rightarrow C_6H_5OH$$

$$C_6H_5OH \rightarrow CO_2 + CO + H_2O$$

Comparing the operational conditions of this study with those of Tezuka and Yajima reveals no significant difference in input power, with 30 W of RF input power and 0.8 mmol min^{-1} of $C_{C_6H_6}$ in the study of Tezuka and Yajima [36], as compared to an RF input power at 40 or 20 W and 2 or 1% (approximately 0.089 or 0.045 mmol min^{-1}) of $C_{C_6H_6}$ in this study. However, $C_{C_6H_6}$ is much less in this study being about 5–10%. Additionally, results of Tezuka and Yajima also demonstrate that phenol yield appeared independent of oxygen flow rate (mmol min^{-1}), implying the presence of oxygen did not affect phenol yield [36]. Accordingly, the main reason why phenol was not found at both O_2/C_6H_6 ratios (7.5 for Fig. 4(A) and 5.0 for (B)) in this study could be the very low $C_{C_6H_6}$. This result indicates that given adequate input power and at low concentrations, C_6H_6 could first be oxidized to phenol, which immediately reacts with oxygen to form other products.

Table 2 clearly shows that when compared with the C_6H_6/Ar system, the addition of 15% of O_2 markedly reduced the yield of PAHs at low input power (40 W). As for the 21 individual PAHs, their Y_{PAH} reduced significantly except for BkF. Total-PAHs were reduced from 1827 to 14.8 μg/g C_6H_6, representing an approximately 99% reduction. Fig. 3 clearly illustrates that comparing yields of PAHs with the same ring number reveals that those in C_6H_6/O_2/Ar system were considerably lower than those in the C_6H_6/Ar system. These analytical results imply that the addition of optimal O_2 helped in decomposing C_6H_6 and effectively suppressed PAHs formation in the RF plasma.

Compared with the C_6H_6/H_2/Ar system, the Y_{PAH} of 19 PAHs species were markedly reduced except for BkF and COR. Comparing yields of PAHs with the same ring number reveals significantly lower yields for those in the C_6H_6/O_2/Ar system compared to the C_6H_6/H_2/Ar system. Total-PAHs reduced from 930 to 14.8 μg/g C_6H_6, representing a reduction of approximately 98.4%. Adding O_2 is clearly superior to adding H_2 in the RF plasma to reduce the yield of PAHs.

During combustion, C_6H_6 reacts with sufficient oxygen to form CO_2 and H_2O.

$$C_6H_6 + 7.5O_2 \rightarrow 6CO_2 + 3H_2O$$

Fig. 4(A) clearly shows that C_6H_6 was thoroughly oxidized to CO_2 (38.3%) and H_2O when the O_2/C_6H_6 ratio was 7.5 (15% of O_2 and 2% of C_6H_6). When the O_2/C_6H_6 ratio was reduced to 5.0 (Fig. 4(B)), other compounds were not found except for CO_2 (23.2%) and H_2O. The above

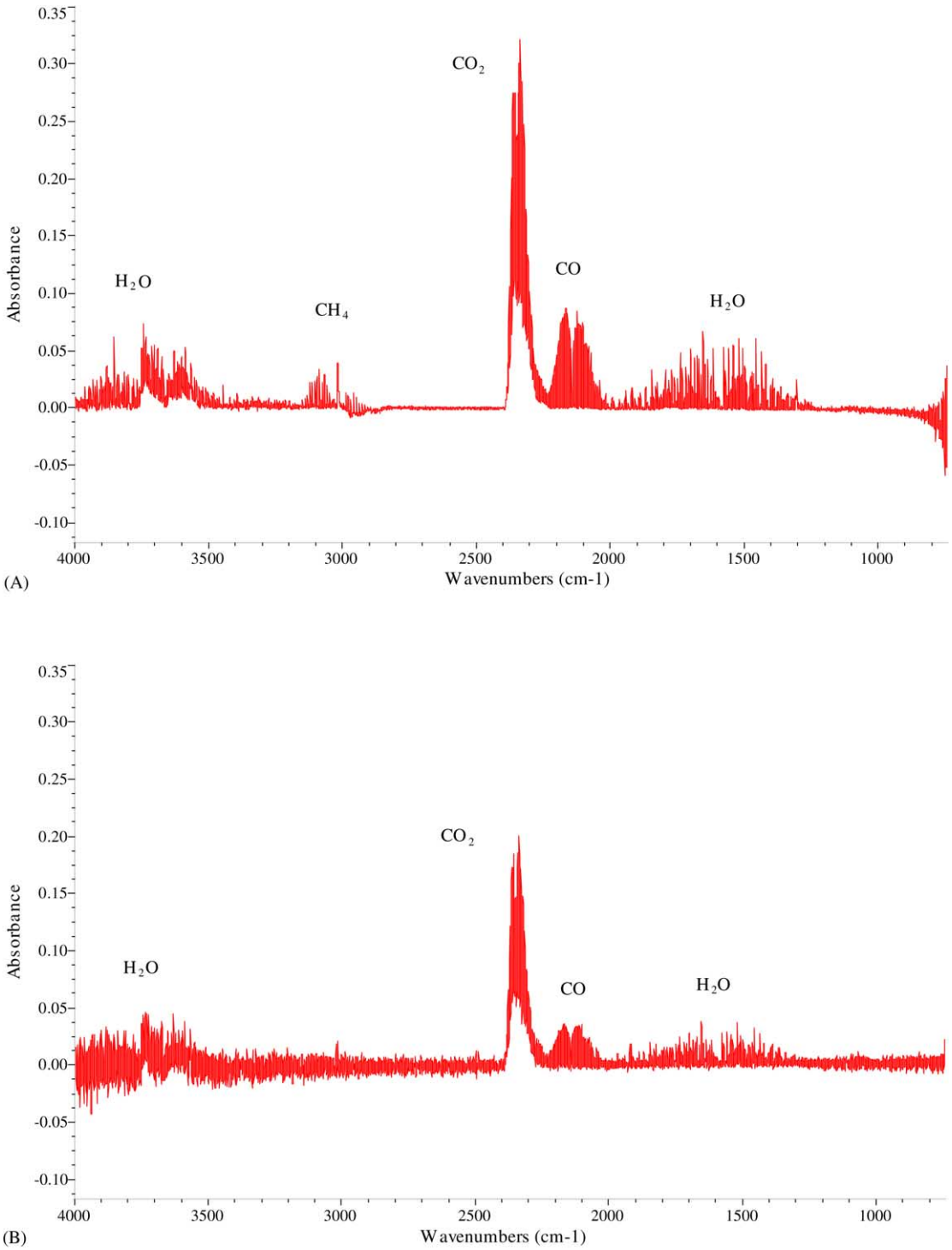

Fig. 4. Spectrum of gaseous products in the C_6H_6/O_2/Ar RF plasma environment. (A) 2% of C_6H_6, 40 W of input power and 15% of O_2. (B) 1% of C_6H_6, 20 W of input power and 5% of O_2.

information demonstrates that similarity exists between RF plasma reaction and the combustion process, owing to the complete destruction of C_6H_6 at the O_2/C_6H_6 ratio of stoichiometry. It also shows that RF plasma is superior to the combustion process, because C_6H_6 can be completely destroyed below the stoichiometric ratio of O_2/C_6H_6 (7.5).

3.4. Phase distribution

PAHs are semi-volatile organic compounds. At room temperature, SVOCs simultaneously exist as gas- and particle-phase and maintain equilibrium. Temperature is the main influence on the phase distribution of PAHs. In the atmosphere,

2- and 3-ring PAHs exist in the gas-phase, but only small amounts are adsorbed onto particles. This phenomenon is more notable during the hot summer. Four-ring atmospheric PAHs also exist primarily in the gas-phase. However, their concentrations in the particle-phase remain higher than those of 3-ring. As for 5-, 6- or 7-ring PAHs in the atmosphere, they all exist primarily in the particle-phase [31–32].

As previously noted, temperature is the primary influence on PAHs distribution between the gas- and particle-phases. PAHs are dominant in the gas-phase at high temperature, and the energetic electrons in RF plasma could result in high temperatures up to 8200 K [29–30], which indicates the importance of gas-phase distribution in the RF plasma environments. However, Hsieh et al. ignored the gas phase PAHs and examined only the PAHs involved in the deposition in the RF plasma. To achieve a full picture of PAHs formation in the RF plasma, PAHs in both the gas- and particle-phase were collected simultaneously and analyzed separately here. Discussion in the earlier parts of this study was based on the combination of gas- and particle-phase of PAHs.

The phase distribution of a PAH describes how a certain PAH is distributed between the gas- and particle- phases. Thus, the gas-phase distribution (%) of each PAH is defined as: [gas-phase Y_{PAH}/(gas-phase Y_{PAH} + particle-phase Y_{PAH})] × 100%, and the particle-phase distribution (%) thus is: (100 − gas-phase distribution) (%). Table 3 lists the phase distributions of individual PAHs and total-PAHs with different input power and feed concentration of C_6H_6 in the C_6H_6/Ar system. As was observed in the atmosphere, 2- and 3-ring PAHs, including Nap, AcPy, AcP, Flu, PA and Ant, existed mainly in the gas-phase under all operational conditions in the C_6H_6/Ar system. Notably, gas-phase distribution of Nap was up in 94.1–99.2% range. On the other hand, the particle-phase distribution of 4-ring PAHs, including FL, Pyr, BaA and CHR, approached 100%. The particle-phase distributions of 5-, 6- and 7-ring PAHs exceeded those of 4-ring. Furthermore, these patterns of phase distribution closely resembled those found in the atmosphere.

In terms of total-PAHs, at low input power (40 W), the gas-phase distribution increased slightly, from 22.8 to 29.8%, as $C_{C_6H_6}$ increased from 1 to 10%. The effect of $C_{C_6H_6}$ on phase distribution was insignificant at low input power. However, at high input power (90 W) the gas-phase distribution increased markedly from 13.3 to 87.2% as $C_{C_6H_6}$ increased from 1 to 10%. These observation results further proved the importance and necessity of measuring PAHs in the gas-phase when high power is used in the C_6H_6/Ar system.

Table 4 lists the comparisons of phase distribution among C_6H_6/Ar, C_6H_6/H_2/Ar and C_6H_6/O_2/Ar systems at 2% of $C_{C_6H_6}$ and 40 W of input power. Regarding individual PAHs, the gas-phase distribution of 2- and 3-ring PAHs was significantly dominant in both the C_6H_6/Ar and C_6H_6/H_2/Ar

Table 3
Phase distributions (%) of individual PAHs and total-PAHs with different input power and feed concentrations of C_6H_6 in the C_6H_6/Ar RF plasma environment

PAHs	40 W				90 W			
	1% C_6H_6		10% C_6H_6		1% C_6H_6		10% C_6H_6	
	Gas-phase (%)	Particle-phase (%)	Gas-phase (%)	Particle-phase (%)	Gas-phase (%)	Particle-phase (%)	Gas-phase (%)	Particle-phase (%)
Nap	94.1	5.9	98.4	1.6	94.0	6.0	99.2	0.8
AcPy	85.1	14.9	91.9	8.1	91.4	8.6	98.5	1.5
AcP	85.2	14.8	89.6	10.4	45.4	54.6	94.3	5.7
Flu	34.9	65.1	69.4	30.6	20.5	79.5	92.8	7.2
PA	13.3	86.7	29.1	70.9	9.9	90.1	93.6	6.4
Ant	7.5	92.5	28.9	71.1	5.7	94.3	85.4	14.6
FL	2.4	97.6	12.3	87.7	2.3	97.7	43.3	56.7
Pyr	20.8	79.2	11.1	88.9	2.2	97.8	36.9	63.1
CYC	0.0	100.0	5.7	94.3	0.3	99.7	5.0	95.0
BaA	0.1	99.9	32.7	67.3	0.0	100.0	5.4	94.6
CHR	0.0	100.0	3.9	96.1	0.9	99.1	9.2	90.8
BbF	2.8	97.2	5.3	94.7	2.4	97.6	7.9	92.1
BkF	ND	ND	ND	ND	100.0	0.0	ND	ND
BeP	0.0	100.0	9.6	90.4	0.7	99.3	1.5	98.5
BaP	0.0	100.0	5.4	94.6	0.5	99.5	2.0	98.0
PER	0.0	100.0	8.0	92.0	ND	ND	0.0	100.0
IND	0.0	100.0	7.0	93.0	0.0	100.0	0.0	100.0
DBA	0.0	100.0	ND	ND	ND	ND	ND	ND
BbC	ND	ND	100.0	0.0	ND	ND	ND	ND
BghiP	0.0	100.0	7.2	92.8	0.8	99.2	0.0	100.0
COR	0.0	100.0	42.0	58.0	0.1	99.9	0.0	100.0
Total-PAHs	22.8	77.2	29.8	70.2	13.3	86.7	87.2	12.8

ND: not detected.

Table 4
Phase distributions (%) of individual PAH and total-PAHs in the C_6H_6[a]/Ar, C_6H_6[a]/H_2/Ar and C_6H_6[a]/O_2/Ar RF plasma environments

PAHs	40 W					
	C_6H_6/Ar		C_6H_6/H_2/Ar		C_6H_6/O_2/Ar	
	Gas-phase (%)	Particle-phase (%)	Gas-phase (%)	Particle-phase (%)	Gas-phase (%)	Particle-phase (%)
Nap	98.6	1.4	97.1	2.9	96.6	3.4
AcPy	81.5	18.5	82.7	17.3	98.9	1.1
Acp	79.6	20.4	70.6	29.4	99.6	0.4
Flu	39.6	60.4	39.0	61.0	98.9	1.1
PA	4.3	95.7	6.4	93.6	96.9	3.1
Ant	4.7	95.3	6.9	93.1	96.7	3.3
FL	0.1	99.9	1.3	98.7	81.3	18.7
Pyr	0.1	99.9	1.3	98.7	90.7	9.3
CYC	0.0	100.0	0.0	100.0	29.0	71.0
BaA	0.0	100.0	0.3	99.7	32.6	67.4
CHR	0.0	100.0	0.0	100.0	76.5	23.5
BbF	0.0	100.0	0.5	99.5	40.1	59.9
BkF	ND	ND	ND	ND	100.0	0.0
BeP	0.1	99.9	0.1	99.9	0.0	100.0
BaP	0.0	100.0	0.0	100.0	0.0	100.0
PER	0.0	100.0	ND	ND	ND	ND
IND	0.0	100.0	0.0	100.0	ND	ND
DBA	0.0	100.0	0.0	100.0	ND	ND
BbC	ND	ND	ND	ND	ND	ND
BghiP	0.2	99.8	ND	ND	ND	ND
COR	20.2	79.8	100.0	0.0	100.0	0.0
Total-PAHs	20.0	80.0	30.0	70.0	95.3	4.7

ND: not detected.
[a] C_6H_6 concentration = 2%.

systems. This phenomenon was even more prominent in the C_6H_6/O_2/Ar system, where gas-phase distributions of 2- and 3-ring PAHs were no less than 96.6%. The particle-phase distribution of 4-ring PAHs were significantly dominant in both C_6H_6/Ar and C_6H_6/H_2/Ar systems, and were 98.7% or higher. In the C_6H_6/O_2/Ar system, the gas-phase distribution of FL, Pyr and CHR was between 76.5 and 90.7%, while that of BaA was 32.6%. Furthermore, the phase distributions for 5-, 6- and 7-ring PAHs among these three systems were practically all in the particle-phase. Regarding the gas-phase distributions of total PAHs in these three systems, they were 20.0, 30.0 and 95.3%, respectively. The above result again demonstrates the importance of gas-phase PAHs in the C_6H_6/O_2/Ar system.

As illustrated in Tables 3 and 4, at least 13.3% amount of PAHs was distributed in gas-phase under all operational conditions. At high $C_{C_6H_6}$ (10%) and high input power (90 W), the gas-phase distribution increases to 87.2%, while in the C_6H_6/O_2/Ar system, the gas-phase distribution increases to 95.3%. The above results indicated that gas-phase PAHs from C_6H_6 should not be ignored in the RF plasma, particularly when a high input power is used in the C_6H_6/O_2/Ar system. Practically, these gas-phase PAHs should be removed using air pollutants control devices, for example, activated carbons.

4. Conclusions

(1) Regarding individual PAH, in the C_6H_6/Ar system, naphthalene ($C_{10}H_8$) was the predominant species found among the 21 PAHs produced under all the operational conditions, and were followed by phenanthrene and chrysene. High-ring PAHs, such as BaP, DBA and BbF, did not form easily under high input power and high $C_{C_6H_6}$.
(2) In the C_6H_6/Ar system, increasing $C_{C_6H_6}$ markedly increases the Y_{PAH} at low input power, but decreases Y_{PAH} slightly at high input power. Simultaneously, based on the same $C_{C_6H_6}$, individual PAHs were significantly fewer at high input power than at low input power. The above information indicate that energetic electrons in the RF plasma were unfavorable for PAH formation. Y_{PAH} decrease with increasing ring number.
(3) In the C_6H_6/H_2/Ar system, Nap, PA and CHR remained the predominant species. Moreover, Y_{PAH} decreased with increasing ring number. As compared to the C_6H_6/Ar system, individual PAHs decreased significantly. Too numerous H_2 molecules would react to form gaseous products, for example C_2H_2, C_2H_4, C_2H_6 and CH_4, which was unfavorable for PAH formation.
(4) In the C_6H_6/O_2/Ar system, C_6H_5OH were not detected in the gas products. Phenoxy pathway may not be the main

mechanism for PAH formation, small quantities of PAHs should be created by the HACA mechanism. Compared with the C_6H_6/Ar and C_6H_6/H_2/Ar systems, PAH yields decreased substantially. These results demonstrate that the addition of O_2 helped to decompose C_6H_6 and reduce PAH formation.

(5) Among C_6H_6/Ar, C_6H_6/H_2/Ar and C_6H_6/O_2/Ar systems, the gas-phase distribution of total-PAHs represented 20–95.3% at 2% of $C_{C_6H_6}$. Additionally, it increased further to 87.2% at 10% of $C_{C_6H_6}$ and high input power (90 W). Therefore, this study suggests that gas-phase PAHs should not be ignored, particularly in C_6H_6/O_2/Ar systems with high input power.

References

[1] R.S. Slysh, C.R. Kinney, Some kinetics of the carbonization of benzene, acetylene and diacetylene at 1200°, J. Phys. Chem. 65 (1961) 1044–1045.

[2] H.J. Singh, R.D. Kern, Pyrolysis of benzene behind reflected shock waves, Combust. Flame 54 (1983) 49–59.

[3] R.D. Smith, A.L. Johnson, Mass spectrometric study of the high temperature chemistry of benzene, Combust. Flame 51 (1983) 1–22.

[4] S.H. Bauer, C.F. Aten, Absorption spectra of polyatomic molecules at high temperatures. II. Benzene and perfluorobenzene. Kinetics of the pyrolysis of benzene, J. Chem. Phys. 39 (1963) 1253–1260.

[5] K. Mimura, Synthesis of polycyclic aromatic hydrocarbons from benzene by impact shock: its reaction mechanism and cosmochemical significance, Geochim. Cosmochim. Acta 59 (1995) 579–591.

[6] F. Cataldo, Ultrasound-induced cracking and pyrolysis of some aromatic and naphthenic hydrocarbons, Ultrason. Sonochem. 7 (2000) 35–43.

[7] C.S. McEnally, L.D. Pfefferle, The effects of slight premixing on fuel decomposition and hydrocarbon growth in benzene-doped methane nonpremixed flames, Combust. Flame 129 (2002) 305–323.

[8] A. Ogata, K. Yamanouchi, K. Mizuno, S. Kushiyama, T. Yamamoto, Oxidation of dilute benzene in an alumina hybrid plasma reactor at atmospheric pressure, Plasma Chem. Plasma Process. 19 (1999) 383–394.

[9] H. Richter, W.J. Grieco, J.B. Howard, Formation mechanism of polycyclic aromatic hydrocarbons and fullerenes in premixed benzene flames, Combust. Flame 119 (1999) 1–22.

[10] A. Tregrossi, A. Ciajolo, R. Barbella, The combustion of benzene in rich premixed flames at atmospheric pressure, Combust. Flame 117 (1999) 553–561.

[11] Y. Chai, L.D. Pfefferle, An experimental study of benzene oxidation at fuel-lean and stoichiometric equivalence ratio conditions, Fuel 77 (1998) 313–320.

[12] G. Bermudez, L. Pfefferle, Laser ionization time-of flight mass spectrometry combined with residual gas analysis for the investigation of moderate temperature benzene oxidation, Combust. Flame 100 (1995) 41–51.

[13] R.P. Lindstedt, G. Skevis, Detailed kinetic modeling of premixed benzene flames, Combust. Flame 99 (1994) 551–561.

[14] C.W. Bauschlicher Jr., A. Ricca, Mechanism for polycyclic aromatic hydrocarbon (PAH) growth, Chem. Phys. Lett. 326 (2000) 283–287.

[15] H.Y. Zhang, J.T. Mckinnon, Elementary reaction modeling of high-temperature benzene combustion, Combust. Sci. Technol. 107 (1995) 261–300.

[16] H. Wang, M. Frenklach, A detailed kinetic modeling study of aromatics formation in laminar premixed acetylene and ethylene flames, Combust. Flame 110 (1997) 173–221.

[17] J.A. Mulholland, M. Lu, D.-H. Kim, Pyrolytic growth of polycyclic aromatic hydrocarbons by cyclopentadienyl moieties, Proc. Combust. Inst. 28 (2000) 2593–2599.

[18] L.T. Hsieh, G.C. Fang, H.H. Yang, Y.F. Wang, M.C. Tsao, W.T. Liao, PAHs formation in the depositions in a methyl *tert*-butyl ether/Ar, a methyl *tert*-butyl ether/O_2/Ar and a methyl *tert*-butyl ether/H_2/Ar RF plasma environment, Plasma Chem. Plasma Process. 22 (2002) 639–658.

[19] M. Shih, W.J. Lee, C.H. Tsai, Decomposition of SF_6 in an RF plasma environment, J. Air Waste Manage. Assoc. 52 (2002) 1274–1280.

[20] Y.F. Wang, W.J. Lee, C.Y. Chen, L.T. Hsieh, Reaction mechanism in both a CHF_3/O_2/Ar and CHF_3/H_2/Ar radio frequency plasma environment, Ind. Eng. Chem. Res. 38 (1999) 3199–3210.

[21] S. Senkan, M. Castaldi, Formation of polycyclic aromatic hydrocarbons (PAH) in methane combustion: comparative new results from premixed flames, Combus. Flame 107 (1996) 141–150.

[22] H.H. Mi, W.J. Lee, T.L. Wu, T.C. Lin, L.C. Wang, H.R. Chao, PAH Emission from a gasoline-powered engine, J. Environ. Sci. Health A31 (1996) 1981–2003.

[23] H.L. Sheu, W.J. Lee, C.C. Su, H.R. Chao, Y.C. Fan, Dry deposition of polycyclic aromatic hydrocarbons in ambient air, J. Environ. Eng. Dec. (1996) 1101–1109.

[24] S.I. Shih, T.C. Lin, M. Shih, Decomposition of Benzene in the RF Plasma Environment Part I. Formation of Gaseous Products and Carbon Depositions, Journal of Hazardous Materials, (2004), in press.

[25] N.M. Marinov, W.J. Pitz, C.K. Westbrook, A.M. Vincitore, M.J. Castaldi, S.M. Senkan, C.F. Melius, Aromatic and polycyclic aromatioc hydrocarbon formation in a laminar premixed *n*-butane flame, Combust. Flame 114 (1998) 192–213.

[26] C. Nisbet, P. LaGoy, Toxic equivalency factors (TEFs) for polycyclic aromatic hydrocarbons (PAHs), Regul. Toxicol. Pharmocol. 16 (1992) 290–300.

[27] H.H. Yang, W.J. Lee, H.H. Mi, C.H. Wong, C.B. Chen, PAH emissions influenced by Mn-based additive and turbocharging from a heavy-duty diesel engine, Environ. Int. 24 (1998) 389–403.

[28] C. Gueret, M. Daroux, Billaud Francis, Methane pyrolysis: thermodynamics, Chem. Eng. Sci. 52 (1997) 815–827.

[29] M. Shimozuma, G. Tochitani, H. Tagashira, Optical emission diagnostics of $H_2 + CH_4$ 50Hz − 13.56MHz plasmas for chemical vapor deposition, J. Appl. Phys. 70 (1991) 645–648.

[30] L.T. Hsieh, W.J. Lee, C.Y. Chen, M.B. Chang, H.C. Chang, Converting methane by using an RF plasma reactor, Plasma Chem. Plasma Process. 18 (1998) 215–239.

[31] G. Dorr, M. Hippelein, H. Kaupp, O. Hutzinger, Baseline contamination assessment for a new resource recovery facility in Germany. Part VI. Levels and profiles of polycyclic aromatic hydrocarbons (PAH) in ambient air, Chemosphere 33 (1996) 1569–1578.

[32] K. Gyula, V.P. Zita, R. Gabor, H. Jozsef, Distribution of polycyclic aromatic hydrocarbons on atmospheric aerosol particles of different sizes, Atmos. Res. 46 (1998) 253–261.

[33] H. Wang, M. Frenklach, Calculations of rate coefficients for the chemically activated reactions of acetylene with vinylic and aromatic radicals, J. Phys. Chem. 98 (1994) 11465–11489.

[34] K. Mimura, M. Ohashi, R. Sugisaki, Hydrocarbon Gases, Aromatic hydrocarbons produced by impack shock from frozen benzene: cosmochemical significance, Earth Planet. Sci. Lett. 133 (1995) 265–269.

[35] K.C. Hou, H.B. Palmer, The kinetics of thermal decomposition of benzene in a flow system, J. Phys. Chem. 69 (1965) 863–868.

[36] M. Tezuka, T. Yajima, Oxidation of aromatic hydrocarbons with oxygen in a radiofrequency plasma, Plasma Chem. Plasma Process. 16 (1996) 329–340.

[37] M.P. Cal, M. Schluep, Destruction of benzene with non-thermal plasma in dielectric barrier discharge reactors, Environ. Prog. 20 (2001) 151–156.